NF-κB1 knockout reduces IL6 expression under hypoxia in renal cell carcinoma

Luiz Felipe S. Teixeira[*], Maria Helena Bellini

Centro de Biotecnologia, Instituto de Pesquisas Energéticas e Nucleares, São Paulo, Brazil

ARTICLE INFO

ABSTRACT

Renal cell carcinoma (RCC) is the most common adult renal epithelial cancer, accounting for more than 90% of all renal neoplasms. Clear cell RCC (ccRCC) is the most common subtype of RCC. Most patients with ccRCC have a mutation in the von Hippel-Lindau (*VHL*) tumor suppressor gene, which encodes a protein that downregulates various intracellular proteins, including hypoxia-inducible factor (HIF). Many molecules have been identified to be responsible for the aggressive phenotype of ccRCC, including the transcription factor nuclear factor kappa B (NF-κB). The increase in NF-κB activity observed in RCC is correlated with an increase in angiogenesis markers, such as interleukin 6 (IL-6). In recent years, several groups have demonstrated the functional role of NF-κB1 in RCC tumorigenicity. Herein, we used the CRISPR/Cas-9 technique to obtain an NF-κB1 knockout-human renal adenocarcinoma cell line. Expression of IL-6 at the mRNA and protein levels was analyzed under normoxia and hypoxia by real time-polymerase chain reaction and multiplex assay, respectively. The CRISPR/Cas9 technique was effective in producing 786-0 knockout cells for NF-κB1 (p105/p50), as confirmed by western blot analysis. Suppression of p50 expression in 786-0 single guide RNA (sg)1, 786-0 sg2 and 786-0 sg3 cells downregulated IL-6 mRNA and protein expression under normoxia and hypoxia. The observed decrease in the differential expression of IL-6 in hypoxia/normoxia is suggestive of a change in cellular responsiveness to hypoxia with respect to IL-6.

Introduction

Renal cell carcinoma (RCC) is the most common adult renal epithelial cancer, accounting for more than 90% of all renal neoplasms (1).

RCC occurs most often in individuals between 70–75 years of age, generally affects men more than women, and factors, such as obesity, smoking, hypertension, and genetic alterations, contribute to the development of RCC (2,3). RCC is a clinically pathologically heterogeneous disease that can be classified into the following types: clear cell, papillary, chromophobic, collecting duct carcinoma, and unclassified (1). Clear cell RCC (ccRCC) is the most common type of RCC, accounting for 70% of all RCC cases (4). Whereas, papillary, chromophobic, and collecting duct RCC account for 10–15%, 4–6%, and less than 1% of all RCC cases, respectively, and unclassified lesions account for 4–5 % of all RCC cases (1,4). Most patients with ccRCC have a mutation in the von Hippel-Lindau (*VHL*) tumor suppressor gene. The *VHL* gene encodes the VHL protein, which negatively regulates various intracellular proteins, including the hypoxia-inducible factor (HIF). HIF is a heterodimeric transcription factor composed of alpha (α) and beta (β) subunits that regulate the expression of genes that facilitate tissue adaptation to low oxygen pressure. Under normoxic conditions, the VHL protein is involved in the degradation of the HIF-α subunit. Loss of function of the *VHL* gene causes an increase in HIF levels even in normoxic conditions, and consequently, an increase in the transcription of several angiogenic factors, such as vascular endothelial growth factor (VEGF), platelet-derived growth factor (PDGF), vascular endothelial growth factor receptor 2 (VEGFR2), and basic fibroblast growth factor (5,6). Expression of angiogenic factors justifies the intense vascularization often seen in RCC and explains the high prevalence of metastasis (30–40% of cases) at the initial diagnosis of the disease (7).

The prognostic value of soluble factors, such as interleukin 6 (IL-6), has been explored. IL-6 is an inflammatory and angiogenic cytokine that acts as an autocrine tumor growth factor, which induces a transcriptional inflammatory response, promoting tumor progression through the Janus kinase (JAK)- signal transducer and activator of transcription (STAT) pathway and inducing tumor angiogenesis by activating the JAK/STAT and phosphoinositide 3-kinase (PI3K)/Akt signaling pathways (8). Clinically, circulating IL-6 level is an important independent prognostic factor in patients with metastatic RCC (9). Zhang et al. demonstrated that STAT3 is a key regulator of the *VEGF* gene; in addition to being a direct activator of the *VEGF* promoter, STAT3 is also involved in PI3K-Akt-mediated HIF-1 expression. Moreover, HIF-1 is a key regulator of the *VEGF* gene (10).

Nuclear factor kappa B (NF-κB) was discovered in 1986 by Sen and Baltimore and was described as a nuclear factor that binds to promoter elements of the light chain of activated B-cell immunoglobulin (11). Subsequent research confirmed that this transcription factor is expressed in almost all cell types and regulates many genes involved in various pathological processes, such as inflammation

* Corresponding author. Email: lfelipetx@gmail.com

and immune response, oxidative stress, carcinogenesis, cell survival, and apoptosis (12).

NF-κB is a pleiotropic transcription factor belonging to the Rel/NF-κB family, which participates in the activation of many genes, including cytokines, metalloproteinases (MMPs), VEGF, Bcl-2, and Bax. In mammals, the Rel family is comprised of five proteins: RelA (p65), RelB, c-Rel, NF-κB1 p105/p50 and NF-κB2 p100/p52. NF-κB proteins can be classified into two groups: the first group includes the p65, RelB, and c-Rel subunits that contain a transactivation domain at the C-terminus and are synthesized in their mature form; and the second group, which is composed of NF-κB1 p105/p50 and NF-κB2 p100/p52 proteins that are synthesized as precursor molecules, which undergo cleavage of the N-terminal region in the proteasome (26S) to generate mature proteins (p50 and p52) (13,14).

All Rel subunits have an N-terminal domain of approximately 300 amino acids called the Rel homology domain, which mediates DNA binding and subunit dimerization. RelA (p65), RelB, and c-Rel contain transactivation domains in their C-terminal region that generally allow dimers containing these subunits to induce gene expression. This domain is also the site of several post-translational regulatory modifications including phosphorylation, acetylation, and nitrosylation. In contrast, NF-kB1 (p105/p50) and NF-kB2 (p100/p52), which undergo proteolysis to produce the DNA-binding isoforms p50 and p52, do not have transactivation domains. Consequently, these p50 or p52 homodimers are generally viewed as transcriptionally inert, i.e., they have DNA-binding capacity but cannot activate gene expression; there are, of course, exceptions (14). There are two pathways of NF-κB p50 activation: the canonical pathway and the noncanonical pathway, which has not yet been fully elucidated (15). The canonical pathway, also known as the classical pathway, is activated by viral infections and inflammatory cytokines. When this pathway is activated, IκB kinase phosphorylates an inhibitor of NF-κB (IκB) protein that is subsequently ubiquitinated and degraded by the proteasome. The free subunits (p65 and p50) of NF-κB translocate to the nucleus, where they induce the transcription of specific genes. In the noncanonical pathway, p50 or p52 homodimers translocate to the nucleus, where they interact with Bcl-3, which has a transactivation domain, and induce gene transcription. These subunits heterodimerize or homodimerize to form activating (p50/p65) and repressing (p50/p50 and p52/p52) dimers, respectively. Without stimulation, NF-κB remains in the cytoplasm in its inactive form bound to an IkB protein, such as IkB-α, IkB-β, IkBγ, IkBδ, and Bcl-3 (13,16).

The connection between the NF-κB and HIF signaling pathways has been proposed by several authors. Studies have shown that NF-κB subunits are linked to the *HIF-1α* promoter and their depletion results in reduced basal le-

vels of *HIF-1α* mRNA. Furthermore, the authors showed that the induction of NF-κB by tumor necrosis factor promotes an increase in the expression and activity of HIF-1α under hypoxic conditions [17-20]. In summary, hypoxia promotes the activation of NF-kB, which subsequently upregulates *HIF-α* transcription, which activates the transcription of genes responsible for the adaptive response to hypoxia. Therefore, in the present study, we aimed to evaluate the impact of *NF-κB1* gene knockout on angiogenesis. We measured the expression of IL-6 in human renal adenocarcinoma cells under normoxic and hypoxic conditions for the same.

Materials and Methods

Cell culture

The human clear cell renal adenocarcinoma with *VHL* gene mutation, 786-0, was purchased from the American Type Culture Collection (ATCC®CRL-1932; Manassas, VA, USA). Cells were cultured in Roswell Park Memorial Institute (RPMI)-1640 medium (Life Technologies, Carlsbad, CA, USA) supplemented with 10% fetal bovine serum (FBS), 100 U/mL penicillin, and 100 μg/mL streptomycin (all obtained from Gibco, Waltham, MA, USA) in a humidified incubator with 5% CO_2 at 37 °C.

NF-κB1 gene knockout

For knockout of the *NF-κB1* gene, the CRISPR-Cas9 technique was used, and the three single guides RNA (sgRNA) sequences used in the present study were designed using the Broad Institute sgRNA Design tool (portals.broadinstitute.org/gpp/public/analysis-tools/sgrna–design). A scrambled control sequence (mock) was designed. The sequences used are listed in Table 1. The lentiCRISPR v2 vector, provided kindly by Dr. Matheus Henrique Dos S. Dias, Special Laboratory of Applied Toxinology, Center for Toxins, Immune Response and Cell Signaling, Instituto Butantan, São Paulo, Brazil (Addgene Plasmid #52961), was used to clone sgRNA sequences following the protocol described by Sanjana et al. (2014) (21,22).

After transformation into *Escherichia coli* DH5α (Subcloning Efficiency DH5α Competent Cells; Invitrogen, Waltham, MA, USA), a two-plasmid system was used to pack the virus particles (pSPAX2-y PSI and pCMV-VsVg; Addgene, Watertown, MA, USA), and the lentiviral particles were cotransfected into HEK 293T cells with the constructed lentiviral interference vectors using Lipofectamine® 2000 (Invitrogen). The virus supernatant was collected 48 h after transfection.

786-0 cells were seeded in six-well plates at 5×10^4 cells per plate in a medium containing lentivirus with NF-kB1–sgRNA or scrambled-sgRNA and polybrene (hexadimethrine bromide; Sigma-Aldrich, St. Louis, MO, USA). After 6 h, the medium containing 10% FBS was refreshed,

Table 1 . Plasmid vector sequences (single guide RNA).

Clones	Sequences
sgRNA NF-κB1 1 (sg1)	5′ – ACTGGAAGCACGAATGACAG – 3′
sgRNA NF-κB1 2 (sg2)	5′ – TTGTCTATGAACATCTGTGG – 3′
sgRNA NF-κB1 3 (sg3)	5′ – AAGTAGGAAATCCATAGTGT – 3′
Scramble/ empty vector (Mock)	5′ – GACCCCCTCCACCCCGCCTC – 3′

Abbreviations: NF-κB, nuclear factor kappa B; sgRNA, single guide RNA.

and after 48 h, puromycin (Invitrogen) was added to select infected cells. The cells were divided into three groups: 786-0-wild type (WT; cells without viral transfection), 786-0-mock (empty vector-transfected control cells), and Renca-shRNA-NF-kB1 (cells transfected with lentivirus NF-kB1-sgRNA).

Cell culture in hypoxia

For the hypoxia assay, approximately 2×10^5 cells were seeded in 60 mm dishes the day before the assay was performed. Cells were incubated for 6 h in a humid hypoxia chamber (StemCellTM Technologies, Vancouver, Canada), with an atmosphere of 1% O_2, 5% CO_2, and 94% N_2 at 37 °C [23]. An O_2 Altair PRO single gas detector (Code:217597, MSA Safety, Cranberry Township, PA, USA) was used to measure O_2 concentration in the hypoxia chamber.

RNA extraction and quantitative real-time reverse transcriptase polymerase chain reaction (qRT-PCR)

Total cellular RNA was extracted using the RNeasy Mini Kit (Qiagen, Valencia, CA, USA). cDNA was then synthesized using the QuantiTect® Reverse Transcription Kit (Qiagen, Hilden, Germany) according to the manufacturer's protocol using 2 μg of RNA and was stored at −20 °C. The Absolute SYBR Green qPCR Mix® (Invitrogen) was used for qRT-PCR according to the manufacturer's instructions. Reactions were carried out in 10 μL and the following PCR conditions were used: 40 cycles of denaturation at 95 °C for 15 s, annealing at 60 °C for 1 h, and elongation at 72 °C for 1 min. The target gene expression levels were normalized to transferrin receptor (*TFRC*) mRNA levels. The primers used were as follows: *IL-6*, 5′-ATTCCTCCCCGCATCA-3′ (forward) and 5′-CAGAGGGGCCTACCCTTAGC-3′ (reverse); *TFRC*, 5′-GGAGGACGCGCTAGTGTTCT-3′ (forward) and 5′-TGCTGATCTAGCTTGATCCATCA-3′ (reverse). Relative gene expression was quantified using the $2^{-\Delta\Delta Ct}$ method [24]. PCR was performed using an ABI-Prism 7000 quantitative PCR system (Applied Biosystems, Foster City, CA, USA).

Protein extraction and western blot analysis

Proteins were extracted from cells using CelLyticTM M (Sigma-Aldrich). After centrifugation at 20.000 × g at 4 ºC for 15 min, the supernatant was collected and a protease inhibitor cocktail (Sigma-Aldrich, St. Louis, MO, USA) was added.

Protein concentration was determined using the bicinchoninic acid method, and protein samples were stored at −80 °C until use in experiments. Proteins (40 μg per lane) were separated by 12% sodium dodecyl sulfate-polyacrylamide gel electrophoresis (SDS-PAGE) and transferred onto polyvinyl difluoride (PVDF) membrane (Thermo Fisher Scientific, Waltham, MA, USA)), which were then blocked in 5% skim milk in Tris-buffered saline at room temperature for 1 h. Membranes were then incubated overnight at 4 °C with the following primary antibodies (all diluted 1: 500): anti-NF-kB1 p105/p50 (ab32360, rabbit monoclonal, Abcam, Cambridge, UK), EPAS-1/HIF-2α (sc-46691, mouse monoclonal, Santa Cruz, Dallas, TX, USA), and anti-β-actin (ab123020, mouse monoclonal, Abcam). Membranes were then incubated with goat or mouse horseradish peroxidase-conjugated secondary antibodies (diluted 1:1,000) for 2 h at room temperature. Immunoreactive protein bands were detected using the SuperSignal® West Pico Chemiluminescent Substrate Kit (Thermo Fisher Scientific, Waltham, MA, USA). Images were acquired using Uvitec Cambridge Alliance 4.7 (Uvitec Cambridge, Cambridge, UK).

MILLIPLEX assay

IL-6 was quantified using the MILLIPLEX MAP Human Circulating Cancer Biomarker kit (Cat. #HCCBP-1MAG-58K, Merck Millipore, Burlington, MA, USA) following the manufacturer's instructions.

Plate reading and data processing were performed at the Immunology Department of the Institute of Biomedical Sciences (ICB-USP) using Luminex® 200™ – Bio Plex®200 system (Bio-Rad, Hercules, CA, USA).
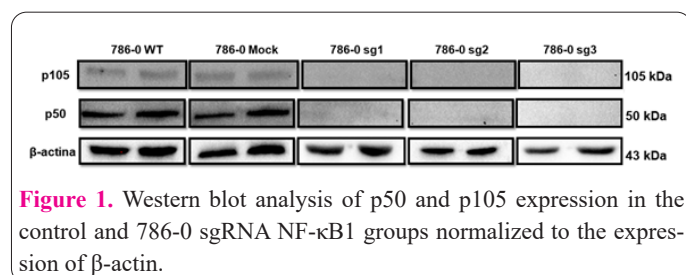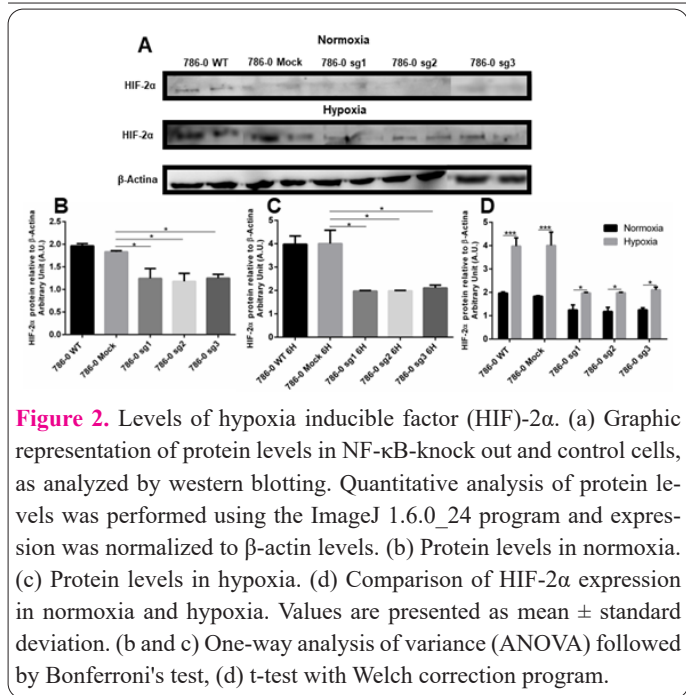
Statistical analysis

Statistical analyses were performed using GraphPad Prism 6.0 (GraphPad Software, Inc., La Jolla, CA, USA). Results are presented as mean ± standard deviation. Statistically significant differences between groups for each assay were analyzed using a one-way analysis of variance, followed by Bonferroni's test. $P < 0.05$ was considered to indicate a statistically significant difference. In the MILLIPLEX assay comparisons between the groups were performed using the chi-square test.

Results

786-0-WT cells and non-target sg-RNA (mock) were used as controls across all experiments. The expression of p50 and p105 proteins was verified in total protein extracts from 786-0 WT, 786-0 mock, 786-0 sg1, 786-0 sg2, and 786-0 sg3 cells. The results showed that the anti-NF-κB1 p105/p50 (ab32360 rabbit monoclonal) antibody was more specific for the p50 portion of NF-kB1, and therefore, this band was used to analyze the efficiency of gene silencing, as shown in Figure 1, the CRISPR/Cas9 technique successfully knocked out the *NF-κB1* gene, resulting in silencing of p50 and p105 protein expression.

HIF-α expression was verified by western blot analysis of total protein extracts (Figure 2a). Under normoxia, HIF-α levels were low, with no difference between the groups (Figure 2b). However, under hypoxia, HIF-α levels increased in all groups, especially in 786-0 WT and 786-0 mock cells. When compared to HIF-2α levels in 786 0-mock cells, the decrease in HIF-2α levels under normoxia was 0.63 ± 0.10-fold, 0.64 ± 0.09-fold, and 0.65 ± 0.11-fold in 786-0 sg1, 786-0 sg2, and 786-0 sg3 cells, respectively (P < 0.05; Figure 2b). Similarly, under hypoxia, the decrease in HIF-2α levels when compared to levels in 786-0-mock cells was 0.50 ± 0.05-fold, 0.51 ± 0.08-fold, and 0.53 ± 0.08-fold in 786-0 sg1, 786-0 sg2, and 786-0

Figure 1. Western blot analysis of p50 and p105 expression in the control and 786-0 sgRNA NF-κB1 groups normalized to the expression of β-actin.

Figure 2. Levels of hypoxia inducible factor (HIF)-2α. (a) Graphic representation of protein levels in NF-κB-knock out and control cells, as analyzed by western blotting. Quantitative analysis of protein levels was performed using the ImageJ 1.6.0_24 program and expression was normalized to β-actin levels. (b) Protein levels in normoxia. (c) Protein levels in hypoxia. (d) Comparison of HIF-2α expression in normoxia and hypoxia. Values are presented as mean ± standard deviation. (b and c) One-way analysis of variance (ANOVA) followed by Bonferroni's test, (d) t-test with Welch correction program.

sg3 cells, respectively (P < 0.05; Figure 2c).

A comparative analysis of HIF-α expression in hypoxic and normoxic conditions is shown in Figure 2d. With regards to the expression of HIF-α in normoxia, 786-0 WT cells showed an increase of 2.02 ± 0.13-fold (P < 0.001), whereas 786-0-mock, 786-0 sg1, 786-0 sg2, and 786-0 sg3 cells showed an increase of 2.19 ± 0.34-fold (P < 0.001), 1.07 ± 0.01-fold (P < 0.05), 1.40 ± 0.18-fold (P < 0.05), and 1.62 ± 0.12-fold (P < 0.05), respectively.

Analysis of *IL-6* mRNA levels

The expression of *IL-6* mRNA in transduced cells under normoxia and hypoxia was analyzed using RT-qPCR. Under both conditions, IL-6 mRNA expression was similar in 786-0 WT and 786-0-mock cells. However, *IL-6* mRNA expression in the knockout cells was lower than that in 786-0-mock cells. The expression of the *IL-6* gene in the knockout cells was significantly lower than that in 786-0-mock cells, both in normoxia (786-0 sg1, 49.03 ± 0.80%; 786-0 sg2, 76.59 ± 12.43%; 786-0 sg3, 66.98 ± 10.89%) and hypoxia (786-0 sg1, 95.85 ± 0.36%; 786-0 sg2, 96.45 ± 0.49%; 786-0 sg3, 91.08 ± 1.42%) (Figure 3a and 3a1).

Analysis of the relative mRNA expression of *IL-6* in normoxia was compared to that in hypoxia. We observed that there was an increase in the expression in all cells, but the 786-0 WT and 786-0-mock cells had a higher expression when compared to that in the transduced cells. Analysis of IL-6 mRNA expression showed that there was an increase in expression in hypoxia, 594.67 ± 108.29 %, 420.74 ± 69.78 %, 168.30 ± 39.09%, 213.90 ± 42.77%, 132.45 ± 36.89%, in 786-0 WT, 786-0 mock, 786-0 sg1, 786-0 sg2, and 786-0 sg3 cells, respectively, compared to that in normoxia (Figure 4).

Analysis of IL-6 protein levels

The levels of IL-6 in the culture medium were evaluated under normoxic and hypoxic conditions. Hypoxia was found to upregulate the expression of IL-6. There was a considerable reduction in IL-6 levels in the culture medium of knock-out cells under normoxia and hypoxia (Figures 3b and 3b1). However, 786-0 sg1 cells had higher
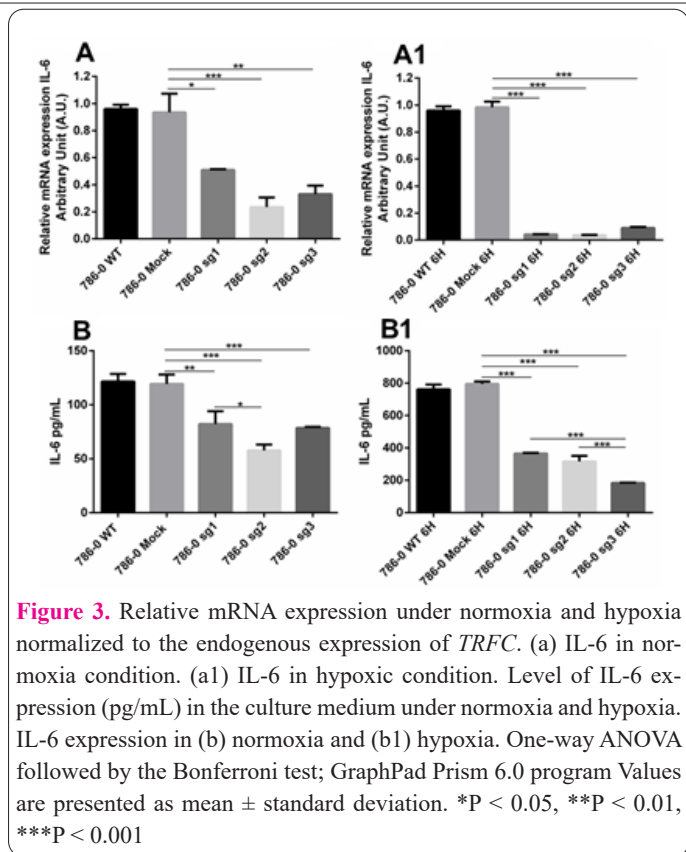
Figure 3. Relative mRNA expression under normoxia and hypoxia normalized to the endogenous expression of *TRFC*. (a) IL-6 in normoxia condition. (a1) IL-6 in hypoxic condition. Level of IL-6 expression (pg/mL) in the culture medium under normoxia and hypoxia. IL-6 expression in (b) normoxia and (b1) hypoxia. One-way ANOVA followed by the Bonferroni test; GraphPad Prism 6.0 program Values are presented as mean ± standard deviation. *P < 0.05, **P < 0.01, ***P < 0.001
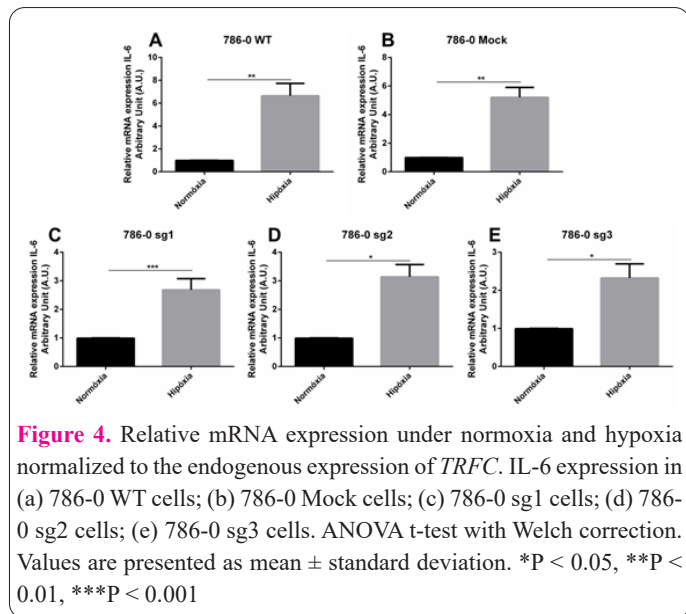
Figure 4. Relative mRNA expression under normoxia and hypoxia normalized to the endogenous expression of *TRFC*. IL-6 expression in (a) 786-0 WT cells; (b) 786-0 Mock cells; (c) 786-0 sg1 cells; (d) 786-0 sg2 cells; (e) 786-0 sg3 cells. ANOVA t-test with Welch correction. Values are presented as mean ± standard deviation. *P < 0.05, **P < 0.01, ***P < 0.001

IL-6 expression than 786-0 sg2 cells under normoxia (P < 0.05). Additionally, under hypoxia, IL-6 levels in 786-0 sg3 cells were significantly lower than those in other cells (P < 0.001).

The data presented in Figures 3b and 3b1 was also used to calculate the differential expression of IL-6 in hypoxia/normoxia. The three groups that were knocked out for NF-κB showed significantly lower differential expression of IL-6 in hypoxia/normoxia compared to that in the control cells (786 sg1 vs 786-0 Mock, P < 0.05; 786 sg2 vs 786-0 mock, P < 0.05, 786 sg3 vs 786-0-mock,- P < 0.001) (Table 2).

Discussion

Hypoxia is a characteristic feature of malignant tumors and is responsible for a cellular adaptive response, which

Table 2. IL-6 expression levels in normoxia and hypoxia. Values are presented as mean ± standard deviation in pg/mL and the differences in expression are presented as fold change.

Cell	Normoxia (pg/mL)	Hypoxia (pg/mL)	Difference in expression (fold change)	P value
786-0 WT	121.62 ± 6.89	761.67 ± 29.61	6.28 ± 0.47	0.6633
786-0 Mock	119.31 ± 8.76	795.62 ± 14.65	6.69 ± 0.36	-
786-0 sg1	82.13 ± 11.94	365.16 ± 4.74	4.50 ± 0.59	< 0.05
786-0 sg2	59.80 ± 5.78	316.74 ± 20.56	4.91 ± 0.19	< 0.05
786-0 sg3	78.55 ± 0.97	183.40 ± 1.66	2.34 ± 0.01	< 0.001

Abbreviations: sg, single guide RNA; WT, wild type.

regulates the expression of genes that affect tumor cell survival, and consequently, tumor progression (25). Hypoxia can activate the NF-κB signal transduction pathway, increasing its binding activity to promoter regions of target genes. Genes activated by the NF-κB pathway allow cells to survive in an environment of low oxygen pressure. In the present study, the expression of NF-κB1, one of the components of the NF-κB dimer, was suppressed in the clear cell adenocarcinoma cell line 786-0 using CRISPR / Cas9 technology.

786-0 cells were transduced with lentiviruses using the VSVG envelope encoding three sgRNA sequences (sgRNA1, sgRNA2, or sgRNA3) for the puromycin resistance cassette. The clones obtained after selection with puromycin were termed 786-0 sg1, 786-0 sg2, and 786-0 sg3. The effectiveness of gene knockout was confirmed by western blot. These results demonstrated that the CRISPR/Cas9 technique is highly effective in editing the clear cell renal tumor lineage. Similar results were obtained by Liu et al. (2020), who used the technique to knockout the epidermal growth factor receptor gene in renal tumor cell lines (26).

Using the clones produced by the CRISPR/Cas9 technique, we verified the effect of NF-κB1 (p105/p50) knockout on the expression of HIF-2α and IL6. The activation of many genes regulated by oxygen pressure (pO$_2$) is mediated by the HIF, a heterodimer composed of the subunits HIF-1α and HIF-1β. Although HIF-1α is the better studied of the HIF-alpha subunit isoforms, recent studies have suggested that HIF-2α is a critical regulator of physiological and pathophysiological angiogenesis and is at least equally important as HIF-1α, HIF-2α regulates several aspects of angiogenesis, including cell proliferation, migration, blood vessel maturation, and metastasis (27). HIF-2α is unstable in normoxia, which explains the low intracellular levels observed in the present study and Albadari et al. (2019) (28).

Despite the low baseline levels, it was possible to verify that NF-κB1 knockout cells showed a significant reduction in the expression of HIF-2α. We attribute this to the fact that the NF-κB signaling pathway is constitutively activated in 786-0 cells, which promotes an imbalance in oxidative metabolism, which in turn, stimulates the production of HIF-2α. The hypoxic microenvironment exacerbates cellular oxidative stress, and consequently, increases HIF-2α expression (29).

IL-6 mRNA and protein levels followed the same trend as HIF-2α mRNA and protein levels in NF-κB1 knockout cells; even in a hypoxic microenvironment that is known to positively regulate these two molecules, significant reductions in mRNA and protein expression were observed. With regards to IL-6, mRNA and protein expression were significantly reduced in NF-κB1 knockout cells. In addition, there was a decrease in the differential expression in hypoxia/normoxia between the NF-κB1 knockout and control cells, suggesting that there was a change in cellular responsiveness to hypoxia with respect to IL-6 expression.

The results of our study are very promising because IL-6 is a prognostic marker for RCC and high plasma IL-6 levels are correlated with therapeutic resistance and reduced patient survival (30,31). These data correlate with and are corroborated by data previously published by our group, where we demonstrated that reduced levels of p50 expression in murine ccRCC led to the downregulation of MMP-9, decreasing the migratory capacity of these cells (32). The effect of IL-6 on cell migration and invasion, mediated by regulation of MMP-2 and MMP-9 expression, was also verified by Sun et al. in nasopharyngeal carcinoma (33).

In summary, the CRISPR/Cas9 technique was effective in producing 786-0 NF-κB1 (p105/p50)-knockout cells. Suppression of p50 expression in 786-0 sg1, 786-0 sg2, and 786-0 sg3 cells resulted in the reduction of IL6 expression under both normoxia and hypoxia. Additionally, the decrease in the differential expression in hypoxia/normoxia suggested a change in cellular responsiveness to hypoxia with respect to IL-6.

Statements & Declarations

Competing interests
The authors have no financial or non-financial interests to disclose.

Author contributions
Data analysis was performed by Luiz Felipe S. Teixeira. The study conception and design were performed by Maria Helena Bellini. All authors contributed to the writing of the manuscript.

Ethical approval
Not applicable

Consent to Participate

Not applicable

Consent to Publish

Not applicable

References

1. Hsieh JJ, Purdue MP, Signoretti S, Swanton C, Albiges L, Schmidinger M, Heng DY, Larkin J, Ficarra V. Renal cell carcinoma. Nat Rev Dis Primers 2017; 3:17009. https://doi.org/10.1038/nrdp.2017.9

2. Weikert S, Ljungberg B. Contemporary epidemiology of renal cell carcinoma: perspectives of primary prevention. World J Urol 2010; 28(3):247–252. https://doi.org/10.1007/s00345-010-0555-1

3. Chow WH, Dong LM, Devesa SS. Epidemiology and risk factors for kidney cancer. Nat Rev Urol 2010; 7(5):245–257. https://doi.org/10.1038/nrurol.2010.46

4. Nardi AC, Zequi Sde C, Clark OA, Almeida JC, Glina S. Epidemiologic characteristics of renal cell carcinoma in Brazil. Int Braz J Urol 2010; 36(2):151–7; discussion 158. https://doi.org/10.1590/s1677-55382010000200004

5. Rini BI, Atkins MB. Resistance to targeted therapy in renal-cell carcinoma. Lancet Oncol 2009; 10(10):992–1000. https://doi.org/10.1016/S1470-2045(09)70240-2

6. Yuen JS. Molecular targeted therapy in advanced renal cell carcinoma: a review of its recent past and a glimpse into the near future. Indian J Urol 2009; 25(4):427–436. https://doi.org/10.4103/0970-1591.57899

7. Harris AL. Hypoxia—a key regulatory factor in tumour growth. Nat Rev Cancer 2002; 2(1):38–47. https://doi.org/10.1038/nrc704

8. Johnson DE, O'Keefe RA, Grandis JR. Targeting the IL-6/JAK/STAT3 signalling axis in cancer. Nature reviews. Clinical oncology 2018; 15(4), 234–248. https://doi.org/10.1038/nrclinonc.2018.8

9. Fu Q, Chang Y, An H, Fu H, Zhu Y, Xu L, Zhang W, Xu J. Prognostic value of interleukin-6 and interleukin-6 receptor in organ-confined clear-cell renal cell carcinoma: a 5-year conditional cancer-specific survival analysis. British journal of cancer 2015; 113(11), 1581–1589. https://doi.org/10.1038/bjc.2015.379

10. Zhang Z, Yao L, Yang J, Wang Z, Du G. PI3K/Akt and HIF-1 signaling pathway in hypoxia-ischemia (Review). Molecular Medicine Reports 2018; 3547-3554. https://doi.org/10.3892/mmr.2018.9375

11. Sen R, Baltimore D. Inducibility of kappa immunoglobulin enhancer-binding protein NF-kappa B by a posttranslational mechanism. Cell 1986; 47(6):921–928. https://doi.org/10.1016/0092-8674(86)90807-x

12. Ghosh S, May MJ, Kopp EB. NF-kappa B and Rel proteins: evolutionarily conserved mediators of immune responses. Annu Rev Immunol 1998; 16:225–260. https://doi.org/10.1146/annurev.immunol.16.1.225

13. Xiao G, Fu J. NF-κB and cancer: a paradigm of Yin-Yang. Am J Cancer Res 2011; 1(2):192–221

14. Cookson VJ, Chapman NR. NF-kappaB function in the human myometrium during pregnancy and parturition. Histol Histopathol 2010; 25(7):945–956. https://doi.org/10.14670/HH-25.945

15. Napetschnig J, Wu H. Molecular basis of NF-κB signaling. Annu Rev Biophys 2013; 42:443–468. https://doi.org/10.1146/annurev-biophys-083012-130338

16. Peng C, Ouyang Y, Lu N, Li N. The NF-κB signaling pathway, the microbiota, and gastrointestinal tumorigenesis: recent advances. Front Immunol 2020; 11:1387. https://doi.org/10.3389/fimmu.2020.01387

17. Görlach A, Bonello S. The cross-talk between NF-kappaB and HIF-1: further evidence for a significant liaison. Biochem J 2008; 412(3):e17–e19. https://doi.org/10.1042/BJ20080920

18. Haase VH. The VHL tumor suppressor: master regulator of HIF. Curr Pharm Des 2009; 15(33):3895–3903. https://doi.org/10.2174/138161209789649394

19. Jeong HJ, Hong SH, Park RK, Shin T, An NH, Kim HM. Hypoxia-induced IL-6 production is associated with activation of MAP kinase, HIF-1, and NF-kappaB on HEI-OC1 cells. Hear Res 2005; 207(1–2):59–67. https://doi.org/10.1016/j.heares.2005.04.003

20. Russo MA, Sansone L, Carnevale I, Limana F, Runci A, Polletta L, Perrone GA, De Santis E, Tafani M. One Special Question to Start with: Can HIF/NFkB be a Target in Inflammation?. Endocr Metab Immune Disord Drug Targets 2015; 15(3), 171–185. https://doi.org/10.2174/1871530315666150316120112

21. Sanjana NE, Shalem O, Zhang F. Improved vectors and genome-wide libraries for CRISPR screening. Nat Methods 2014; 11(8):783–784. https://doi.org/10.1038/nmeth.3047

22. Shalem O, Sanjana NE, Hartenian E, Shi X, Scott DA, Mikkelson T, Heckl D, Ebert BL, Root DE, Doench JG, Zhang F. Genome-scale CRISPR-Cas9 knockout screening in human cells. Science 2014; 343(6166):84–87. https://doi.org/10.1126/science.1247005

23. Wohlrab C, Kuiper C, Vissers MC, Phillips E, Robinson BA, Dachs GU. Ascorbate modulates the hypoxic pathway by increasing intracellular activity of the HIF hydroxylases in renal cell carcinoma cells. Hypoxia (Auckl) 2019; 7:17–31. https://doi.org/10.2147/HP.S201643

24. Livak KJ, Schmittgen TD. Analysis of relative gene expression data using real-time quantitative PCR and the 2(-Delta Delta C(T)) Method. Methods 2001; 25(4):402-408. doi:10.1006/meth.2001.1262

25. Royds JA, Dower SK, Qwarnstrom EE, Lewis CE. Response of tumour cells to hypoxia: role of p53 and NFkB. Mol Pathol 1998; 51(2):55–61. https://doi.org/10.1136/mp.51.2.55

26. Liu B, Diaz Arguello OA, Chen D, Chen S, Saber A, Haisma HJ. CRISPR-mediated ablation of overexpressed EGFR in combination with sunitinib significantly suppresses renal cell carcinoma proliferation. PLOS ONE 2020; 15(5):e0232985. https://doi.org/10.1371/journal.pone.0232985

27. Befani C, Liakos P. The role of hypoxia-inducible factor-2 alpha in angiogenesis. J Cell Physiol 2018; 233(12):9087–9098. https://doi.org/10.1002/jcp.26805

28. Albadari N, Deng S, Li W. The transcriptional factors HIF-1 and HIF-2 and their novel inhibitors in cancer therapy. Expert Opin Drug Discov 2019; 14(7):667–682. https://doi.org/10.1080/17460441.2019.1613370

29. Tam AB, Mercado EL, Hoffmann A, Niwa M. ER stress activates NF-κB by integrating functions of basal IKK activity, IRE1 and PERK. PLOS ONE 2012; 7(10):e45078. https://doi.org/10.1371/journal.pone.0045078

30. Aziziaram, Z., Bilal, I., Zhong, Y., Mahmod, A., Roshandel, M. R. Protective effects of curcumin against naproxen-induced mitochondrial dysfunction in rat kidney tissue. *Cellular, Molecular and Biomedical Reports*, 2021; 1(1): 23-32. https://doi.org/10.55705/cmbr.2021.138879.1001

31. Ishibashi K, Koguchi T, Matsuoka K, Onagi A, Tanji R, Takinami-Honda R, Hoshi S, Onoda M, Kurimura Y, Hata J, Sato Y, Kataoka M, Ogawsa S, Haga N, Kojima Y. Interleukin-6 induces drug resistance in renal cell carcinoma. Fukushima J Med Sci 2018; 64(3):103–110. https://doi.org/10.5387/fms.2018-15

32. Teixeira LFS, Peron JPS, Bellini MH. Silencing of nuclear factor kappa B 1 gene expression inhibits colony formation, cell migration and invasion via the downregulation of interleukin 1 beta

and matrix metallopeptidase 9 in renal cell carcinoma. Mol Biol Rep 2020; 47(2):1143–1151. https://doi.org/10.1007/s11033-019-05212-9

33. Sun W, Liu DB, Li WW, Zhang LL, Long GX, Wang JF, Mei Q, Hu GQ. Interleukin-6 promotes the migration and invasion of nasopharyngeal carcinoma cell lines and upregulates the expression of MMP-2 and MMP-9. Int J Oncol. 2014; 44(5):1551–1560. https://doi.org/10.3892/ijo.2014.2323